J Mol Model (2005) 12: 101–110
DOI 10.1007/s00894-005-0013-y

ORIGINAL PAPER

Matthew C. Lee · Rong Yang · Yong Duan

Comparison between Generalized-Born and Poisson–Boltzmann methods in physics-based scoring functions for protein structure prediction

Received: 17 March 2005 / Accepted: 23 June 2005 / Published online: 12 August 2005

Abstract Continuum solvent models such as Generalized-Born and Poisson–Boltzmann methods hold the promise to treat solvation effect efficiently and to enable rapid scoring of protein structures when they are combined with physics-based energy functions. Yet, direct comparison of these two approaches on large protein data set is lacking. Building on our previous work with a scoring function based on a Generalized-Born (GB) solvation model, and short molecular-dynamics simulations, we further extended the scoring function to compare with the MM-PBSA method to treat the solvent effect. We benchmarked this scoring function against seven publicly available decoy sets. We found that, somewhat surprisingly, the results of MM-PBSA approach are comparable to the previous GB-based scoring function We also discussed the effect to the scoring function accuracy due to presence of large ligands and ions in some native structures of the decoy sets.

Keywords Poisson–Boltzmann continuum solvent model · Protein structure prediction · AMBER force field · Molecular mechanics

Background

In the physics-based approaches, the free energy of a given conformational state, *i*, relative to a chosen reference state in solution can be approximated by two components:

$$\Delta G_i = \Delta G_{\text{internal}} + \Delta G_{\text{solvation}} \quad (1)$$

where $\Delta G_{\text{internal}}$ is the intramolecular free-energy component consisting of internal entropy and internal energies, including bond, angle, torsional, van der Waals and electrostatics energy terms. $\Delta G_{\text{solvation}}$ accounts for the solvation free energy. The term $\Delta G_{\text{internal}}$ is often modeled by molecular mechanics with force fields such as AMBER, [1] OPLS [2] and others. Therefore, the free-energy component $\Delta G_{\text{internal}}$ is often referred to as ΔG_{MM}. The $\Delta G_{\text{solvation}}$ term describes the free energy due to solvation, which includes hydrophobic packing and solvent-solute polarization.

Recent development in physics-based scoring functions has focused on continuum-solvent models that implicitly account for the solvation effect in a mean-field manner. Lazaridis et al. [3, 4] have developed an effective energy function which combines the CHARMM potential energy with a Gaussian model for the solvation free energy to discriminate between correctly folded and misfolded conformations of six proteins. They found that this approach was successful in most cases when combined with energy minimization, but was not successful with molecular-dynamics simulations. Several other authors also developed physics-based scoring functions that incorporated different theoretical treatments of the solvation effect, including a noniterative Langevin dipole solvent, [5] explicit solvent combined with short molecular-dynamics, [6] and implicit solvent based on different implementations of Generalized Born (GB) solvent models. [7–9] Most recently, Hsieh and Luo [10] have also developed a scoring function based on a revised parm99 parameter set of the AMBER force field and a Poisson–Boltzmann implicit solvent treatment of the solvation effect with excellent results, albeit at a higher computational cost. These studies have laid the foundation for physics-based scoring function for protein structure prediction and encouraging results have been obtained.

Generalized-Born and Poisson–Boltzmann (and MM-PBSA) are two of the most important continuum-

M. C. Lee · R. Yang
Department of Chemistry and Biochemistry,
University of Delaware, Newark, DE 19716, USA

Y. Duan (✉)
UC Davis Genome Center and Department of Applied Science,
University of California, Davis, CA 95616, USA
E-mail: duan@ucdavis.edu
Tel.: +1-530-7547632
Fax: +1-530-7549658

solvent methods to treat the solvation effects. Technically, the GB method is considered computationally less intensive. However, solution of the Poisson–Boltzmann equation has been treated as the gold standard and has been the basis for the development of GB parameters. Thus, MM-PBSA method is considered somewhat superior in terms of accuracy although it is expected that these two methods may yield comparable results when GB is parameterized properly. Nevertheless, there are no direct comparisons between these two important methods on large data sets.

Previously, we reported a scoring function based on the Duan et al. [11] AMBER parameter set ff03 with a GB implicit solvent model and short molecular-dynamics simulation. We applied this scoring function to an extensive set of decoys and found that this approach yielded excellent performance with a computationed cost comparable to minimization-based scoring schemes [12]. In this paper, we examine the MM-PBSA [13] method to estimate the solvation free energy and explore the performance of this incremental increase in scoring-function complexity.

The general idea of MM-PBSA is to use molecular dynamics to generate a series of snapshots and then to calculate the average free energy $\Delta\bar{G}$.

$$\Delta\bar{G} = \Delta\overline{E}_{\mathrm{MM}} + \Delta\bar{G}_{\mathrm{PBSA}} - T\Delta S_{\mathrm{MM}}, \qquad (2)$$

where $\Delta\bar{G}$ is the calculated average free energy, $\Delta\overline{E}_{\mathrm{MM}}$ is the average molecular mechanics energy, $\Delta\bar{G}_{\mathrm{PBSA}}$ is the solvation free energy. The $-T\Delta S_{\mathrm{MM}}$ term represents the solute configuration entropy and can be estimated by quasi-harmonic analysis of the trajectory or by normal-mode analysis [13]. $\Delta\bar{G}_{\mathrm{PBSA}}$ is calculated with a numerical solution of the Poisson–Boltzmann equation where the surface-area term is included to estimate the nonpolar free-energy component [14].

Typically, the molecular-dynamics trajectories used for MM-PBSA calculations are generated from explicit solvent simulations [15]. The accuracy of this approach has been demonstrated in several applications such as estimation of the relative free energies of duplex RNA and DNA, [16, 17] and binding free-energy calculations [18, 19]. However, the requirement of full atomic representation of both solute and solvent, even for short molecular dynamics, still presents a substantial computational burden, considering the large number of decoys to be evaluated in any particular prediction application. To reduce the computational requirement further, we elected to substitute the GB model for explicit solvent in generating the molecular-dynamics trajectories. Because the new results are based on the identical set of snapshots generated from earlier GB simulations, we can faithfully compare the two methods.

In addition to this simplification, we also elected to exclude the $-T\Delta S_{\mathrm{MM}}$ term in our scoring function. This choice can be rationalized by noting that the solute entropy comprises two components, including entropy due to a number of conformations and configurational entropy due to the shape of individual conformation. Where the number of conformations is implicitly taken into consideration by the number of decoys, the configurational entropy, which can be calculated by normal-mode analysis, is generally similar from one conformation to another as long as the conformations are relatively compact. Therefore, it is acceptable to ignore the explicit solute entropic terms in the scoring function.

In the remainder of this paper, we present the scoring results of this AMBER/MM-PBSA scoring function as applied to the same set of decoys used in the earlier AMBER/GB-MD scoring-function evaluation.

Methods

Protein decoys were the same as in the previous study. All calculations were performed on our in-house 40 PC dual Pentium IV Beowulf cluster. A set of Perl scripts was developed to automate the preparation of molecular-dynamics simulations and MM-PBSA calculations. The molecular-dynamics simulations were performed by using AMBER7 suite, while the MM-PBSA calculation was calculated by using MM-PBSA scripts in AMBER7 and Delphi.

All decoy structures were prepared with the Leap modules in AMBER and underwent 500 steps of constrained minimization using the Sander module. The minimized structures were then subjected to a 5-ps equilibration followed by another 5-ps molecular-dynamics simulation, both using 2-fs time steps. During the equilibration runs, initial velocities were assigned from a Maxwellian distribution at a temperature equal to 100 K. Both the equilibration and production were kept at a constant temperature of 300 K using Berendsen's weak coupling scheme. Solvent effects were treated with the GB implicit solvent model implemented in the AMBER package using a cutoff value of 200 Å for the nonbonded interaction. The coordinates were saved every 1 ps for MM-PBSA calculation.

The MM-PBSA energy scoring function contains the following terms:

$$E_{\mathrm{PBTOT}} = E_{\mathrm{bond}} + E_{\mathrm{angle}} + E_{\mathrm{dihedral}} + E_{1-4\mathrm{NB}} + E_{1-4\mathrm{EEL}} + E_{\mathrm{vdw}} + E_{\mathrm{elec}} + E_{\mathrm{PBSUR}} + E_{\mathrm{PBCAL}}, \qquad (3)$$

where E_{bond}, E_{angle}, and E_{dihedral} are the bond terms, $E_{1-4\mathrm{NB}}$, $E_{1-4\mathrm{EEL}}$, E_{vdw} and E_{elec} are the nonbonded terms, E_{PBSUR} is the hydrophobic contribution to salvation-free energy for PB calculations and E_{PBCAL} is the reaction-free energy calculated by PB. In our analysis, the PB total energy was calculated for the five snapshots from the short MD production run and the average value E_{PBTOT} was taken as the score. The atomic charges were obtained from Amber ff03 force field. The dielectric constant of the protein was set to 2.0 and that for the surrounding solvent was set to 80.0. The linear PB was calculated iteratively twice. The surface tension was set

to 0.00542 kcal mol^{-1} Å^2. The radius of the probe sphere used to calculate the solvent accessible surface is set as 1.4 Å.

Results and discussion

To facilitate comparison, we carried out the entire two-stage scoring starting from the MD-GB calculation as we had done in our previous study and using the same trajectory generated to perform the MM-PBSA calculations in the second stage. In this study, other than the length of simulations and number of snapshots used in MM-PBSA calculation, we left all other parameters as their default values in the AMBER package. Here we are primarily interested in a straightforward estimation of how well current standard protocols can be applied towards the hierarchical scheme of structure prediction. The results of our scoring are presented in Tables 1, 2, 3, 4, 5, 6, and 7. In the following sections, we examine four types of benchmarking measurements to assess the performance of this scoring function. In the first benchmarking test, we ask the question "How accurately can this new scoring function identify the experimentally determined native structure from the ensemble of decoys?" In the second benchmark, we examine the stability gap-energy fluctuation ratio of the resulting scores. This measure is assessed by the z-scores of the native structures and tells us how much the scoring function separates out the native structure from the rest of the decoys. In the third benchmark, we ask the question of how well the energy scores correlate to similarity distances between decoys and the native structure. And finally, in the fourth benchmark, we look at the per-

Table 1 Ranking statistics of 4-state reduced decoy set

PDB	N_{res}	RMSD	N_{decoy}	PBSA					GB				
				Rank	z	z'	R	R_s	Rank	z	z'	R	R_s
1ctf	68	2.2–10.2	631	1	−3.00	−1.29	0.27	0.48	1	−1.70	−0.73	0.12	0.51
1r69	63	2.3–9.5	676	1	−2.89	−0.90	0.40	0.56	1	−1.89	−0.73	0.23	0.60
1sn3	65	2.5–10.5	661	1	−1.84	−0.70	0.18	0.33	1	−1.14	−0.64	0.09	0.35
2cro	65	2.1–9.7	675	1	−1.99	−0.26	0.43	0.64	1	−1.54	−0.49	0.20	0.58
3icb	75	1.8–10.7	654	*7*	*−1.34*	*0.31*	*0.30*	*0.53*	*2*	*−0.80*	*0.01*	*0.16*	*0.62*
4pti	58	2.8–10.8	688	1	−3.63	−1.13	0.27	0.30	1	−3.46	−1.70	0.28	0.51
4rxn	54	2.6–9.3	678	*6*	*−2.20*	*0.14*	*0.28*	*0.26*	1	−5.00	−1.86	0.49	0.42
Average	64	2.3–10.1	666		−2.41	−0.55	0.30	0.44		−2.22	−0.88	0.22	0.51

Incorrectly identified entries are marked in italics

Table 2 Ranking statistics of fisa decoy set

PDB	N_{res}	RMSD	N_{decoy}	PBSA					GB				
				Rank	z	z'	R	R_s	Rank	z	z'	R	R_s
1ctf	68	2.2–10.2	631	*226*	*−0.09*	*0.64*	*0.02*	*0.07*	*471*	*0.08*	*0.37*	*0.04*	*0.25*
1hdd-C	63	2.3–9.5	676	*229*	*−0.14*	*0.78*	*0.06*	*0.08*	*415*	*0.00*	*0.35*	*0.05*	*0.23*
2cro	65	2.5–10.5	661	1	−1.06	−0.06	0.03	0.18	1	−0.65	−0.26	−0.02	0.07
4icb	65	2.1–9.7	675	*22*	*−0.81*	*0.33*	*0.04*	*0.07*	1	−0.58	−0.10	0.03	0.09
Average	65.3	2.3–10.1	661		−0.53	0.42	0.04	0.10		−0.29	0.09	0.02	0.16

Incorrectly identified entries are marked in italics

Table 3 Ranking statistics of Baker CASP3 decoy set

PDB	N_{res}	RMSD	N_{decoy}	PBSA					GB				
				Rank	z	z'	R	R_s	Rank	z	z'	R	R_s
1bg8-A	76	6.0–15.8	1201	*2*	*−0.87*	*0.12*	*0.02*	*0.11*	1	−0.45	−0.03	0.01	0.07
1bl0	99	3.6–18.2	972	*2*	*−0.77*	*0.00*	*0.00*	*−0.02*	1	−0.53	−0.02	−0.01	−0.07
1eh2	79	4.0–15.3	2414	*1858*	*−0.14*	*0.51*	*0.03*	*−0.04*	*879*	*−0.27*	*0.18*	*0.04*	*−0.01*
1jwe	114	7.8–20.9	1408	1	−1.58	−0.71	0.03	0.09	1	−1.02	−0.48	0.03	0.15
Smd3	71	8.5–17.0	1201	1	−1.65	−0.79	0.05	0.06	1	−0.97	−0.41	0.05	0.10
Average	87.8	6.1–18.6	1439		−1.01	−0.18	0.03	0.04		−0.65	−0.15	0.02	0.05

Incorrectly identified entries are marked in italics

Table 4 Ranking statistics of the Globin Homology (hg_structal) decoy set

PDB	N_{res}	RMSD	N_{decoy}	PBSA					GB				
				Rank	z	z'	R	R_s	Rank	z	z'	R	R_s
1ash	147	2.2∼7.0	30	1	−2.34	−0.88	0.59	0.63	1	−2.85	−1.16	0.34	0.27
1bab-B	146	0.7∼6.9	30	1	−2.76	−1.35	0.70	0.80	1	−2.48	−1.00	0.83	0.89
1col-a	197	12.3∼30.2	30	1	−3.20	−2.27	0.53	0.24	1	−1.53	−1.08	0.27	0.22
1cpc-A	162	6.8∼14.0	30	1	−4.41	−3.71	0.67	0.24	1	−4.42	−3.54	0.60	0.07
1ecd	136	2.5∼6.2	30	1	−0.97	−0.40	0.58	0.56	1	−0.71	−0.34	0.52	0.63
1emy	153	0.7∼9.3	30	1	−1.29	−0.11	0.64	0.91	1	−0.89	−0.14	0.45	0.81
1flp	142	1.7∼7.2	30	1	−2.88	−1.56	0.72	0.50	1	−3.29	−2.50	0.82	0.54
1gdm	153	2.6∼8.4	30	1	−1.17	−0.67	0.59	0.67	1	−0.81	−0.42	0.54	0.66
1hbg	147	2.1∼6.9	30	1	−2.76	−1.65	0.69	0.61	1	−3.23	−1.92	0.75	0.76
1hbh-A	142	1.0∼6.3	30	1	−1.93	−0.71	0.89	0.89	1	−3.23	−1.92	0.74	0.66
1hbh-B	146	1.0∼7.3	30	1	−1.90	−0.44	0.86	0.81	1	−2.01	−0.65	−0.12	−0.08
1hda-A	141	0.5∼5.8	30	1	−1.63	−0.12	0.79	0.83	1	−1.85	−0.23	0.91	0.92
1hda-B	145	0.5∼5.6	30	1	−2.33	−0.83	0.81	0.83	1	−2.11	−0.79	0.88	0.92
1hlb	157	2.9∼7.0	30	*6*	*−0.85*	*0.35*	*0.47*	*0.41*	*5*	*−0.79*	*0.66*	*0.52*	*0.52*
1hlm	158	3.0∼8.7	30	*28*	*0.29*	*0.85*	*0.06*	*0.30*	*29*	*0.15*	*0.64*	*0.04*	*0.30*
1hsy	153	0.8∼9.7	30	*5*	*−0.87*	*0.18*	*0.73*	*0.84*	*2*	*−0.60*	*0.03*	*0.61*	*0.85*
1ith-A	146	1.6∼6.1	30	1	−0.92	−0.09	0.32	0.43	1	−0.55	−0.05	0.18	0.47
1lht	153	0.8∼9.7	30	1	−1.03	−0.01	0.39	0.69	1	−0.69	−0.04	0.22	0.70
1mba	13	1.8∼7.3	30	1	−2.44	−0.63	0.66	0.53	1	−2.61	−1.32	0.82	0.65
1mbs	153	1.7∼9.3	30	*29*	*1.52*	*2.83*	*0.27*	*0.63*	*29*	*0.73*	*1.55*	*0.14*	*0.63*
1myg-A	153	0.5∼9.6	30	*4*	*−0.95*	*0.40*	*0.49*	*0.75*	*4*	*−0.68*	*0.17*	*0.30*	*0.76*
1myj-A	153	0.6∼7.9	30	*4*	*−1.76*	*0.44*	*0.86*	*0.85*	*5*	*−1.57*	*0.42*	*0.89*	*0.84*
1myt	146	1.0∼10.0	30	1	−0.97	−0.01	0.44	0.88	1	−0.72	−0.21	0.30	0.85
2dhb-A	141	0.6∼6.4	30	*8*	*−0.67*	*0.91*	*0.83*	*0.86*	*13*	*−0.41*	*1.37*	*0.81*	*0.86*
2dhb-B	146	0.9∼7.1	30	1	−2.05	−0.09	0.71	0.72	*18*	*0.09*	*2.15*	*0.14*	*0.08*
2lhb	149	3.0∼8.1	30	1	−2.86	−1.54	0.65	0.17	1	−3.06	−1.81	0.28	−0.06
2pgh-A	141	0.7∼6.5	30	*16*	*−0.13*	*1.39*	*0.88*	*0.84*	*14*	*−0.40*	*1.04*	*0.89*	*0.87*
2pgh-B	146	0.8∼7.5	30	*8*	*−0.35*	*0.36*	*0.73*	*0.77*	*8*	*−0.34*	*0.25*	*0.72*	*0.88*
4sdh-A	145	2.3∼6.4	30	1	−2.83	−1.47	0.67	0.46	1	−3.47	−2.23	0.64	0.31
Average	150	2.0∼8.6	30		−1.60	−0.37	0.63	0.64		−1.53	−0.45	0.52	0.58

Incorrectly identified entries are marked in italics

Table 5 Ranking statistics of the lattice fit

PDB	N_{res}	RMSD	N_{decoy}	PBSA					GB				
				Rank	z	z'	R	R_s	Rank	z	z'	R	R_s
1beo	98	7.0∼15.6	2001	1	−4.57	−2.62	0.00	0.01	1	−2.87	−1.40	−0.03	−0.05
1ctf	68	5.5∼12.8	2001	1	−4.91	−2.65	−0.06	−0.11	1	−2.33	−1.21	−0.05	−0.13
1dkt-A	72	6.7∼14.1	2001	1	−2.42	−1.27	−0.01	−0.07	1	−1.05	−0.25	−0.02	−0.11
1fca	55	5.1∼11.4	2001	1	−1.14	−0.11	0.02	0.01	1	−1.14	−0.62	0.02	−0.03
1nkl	78	5.3∼13.6	2001	1	−1.64	−0.12	0.07	0.43	*3*	*−1.05*	*0.13*	*0.00*	*0.33*
1pgb	56	5.8∼12.9	2001	1	−1.69	−0.89	−0.01	0.04	1	−0.82	−0.42	−0.02	0.04
1trl-A	62	5.4∼12.5	2001	1	−1.95	−0.87	0.02	0.16	1	−0.94	−0.24	0.01	0.12
Average	70	5.8∼13.3	2001		−2.62	−1.22	0.01	0.07		−1.46	−0.57	−0.01	0.02

Incorrectly identified entries are marked in italics

formance in comparison to the scoring function of Hiseh and Luo, in which the PBSA treatment was directly incorporated into the molecular-dynamics simulation as opposed to our post-processing approach.

Native structure identification

The ultimate goal of developing scoring functions is to identify the most native-like structure from an ensemble of decoys. The accuracy of the PBSA scoring function (percentage of correctly identified structures in a set) ranges from the low of 25% to the high of 100%. Out of a total of 115 decoy ensembles scored, the PBSA scoring function incorrectly identified the native structure in 20 (17%) instances, whereas the GB scoring function performed slightly better with 17 (15%) instances of incorrect identification. However, the failures in each case do not overlap completely. In Table 8, we summarize the structures incorrectly identified by each scoring function in a side-by-side comparison. Because the performance of energy-scoring functions is typically

Table 6 Ranking statistics of local minima decoy set (LMDS)

PDB	N_{res}	RMSD	N_{decoy}	PBSA					GB				
				Rank	z	z'	R	R_s	Rank	z	z'	R	R_s
1bo0n-B	31	2.45–6.03	498	*141*	*−0.55*	*2.54*	*0.06*	*0.08*	*211*	*−0.20*	*2.18*	*0.10*	*0.10*
1bba	36	2.78–8.91	501	*478*	*0.44*	*1.15*	*−0.05*	*−0.07*	*501*	*10.57*	*13.49*	*−0.04*	*0.07*
1ctf	68	3.59–12.5	498	1	−3.21	−1.24	0.34	0.37	1	−6.02	−3.07	0.31	0.28
1dtk	57	4.32–12.6	216	*104*	*−0.04*	*2.68*	*0.07*	*0.06*	1	−5.20	−2.31	0.11	−0.01
1fc2	43	3.99–8.45	501	1	−3.07	−0.18	0.02	0.01	*21*	*−1.84*	*1.18*	*−0.01*	*−0.02*
1igd	61	3.11–12.6	501	1	−2.86	−1.05	0.05	0.04	1	−6.41	−3.91	0.10	0.00
1shf-A	59	4.39–12.3	438	1	−2.86	−1.05	0.03	0.03	1	−6.41	−3.91	0.08	0.07
2cro	65	3.87–13.5	501	1	−2.16	−0.54	0.17	0.17	1	−7.56	−4.66	0.10	0.00
2ovo	56	4.38–13.4	348	1	−2.73	−0.85	0.07	−0.03	1	−5.55	−3.00	−0.03	−0.04
4pti	58	4.94–13.2	344	1	−4.21	−1.89	−0.07	−0.12	1	−7.77	−5.36	0.10	0.00
Average	53	3.48–11.3	435		−2.12	−0.04	0.07	0.05		−3.64	−0.94	0.08	0.05

Incorrectly identified entries are marked in italics

coupled to the method of decoy generation, we further compared the performances of the scoring functions in each of the seven decoy sets.

In the first set containing ab initio models generated by the 4-state reduced method of Park and Levitt [20], both the GB and PBSA scoring functions incorrectly identified the native structure of 3icb, a calcium-binding protein from bovine intestine. However, the native structures were still ranked among the top ten structures and the top-ranking decoy was only less than 2.8 Å away from the native structure. PBSA also incorrectly identified 4rxn, an oxidized rubredoxin. Figure 1 shows the native structures of 3icb and 4rxn. In both cases, metal ions played integral roles in the native structures. Thus, explicit consideration of the ions is necessary. Unfortunately, neither of our scoring functions considered the energetic contributions of the bound ions.

In the fisa set, which contains decoys for four small α-helical proteins, both GB and PBSA failed on 1fc2 and 1hdd-C. PBSA also failed on 4icb. In the case of 1fc2, a human Fc fragment, the native structure obtained from PDB is a complex structure with fragment B of protein A bound to it. The top-ranking decoy is 3.98 Å away by GB and 8.7 Å away by PBSA. In the case of 1hdd-C, the experimental structure is in complex with DNA, and both GB and PBSA identified the same decoy structure (6.005 Å away from the native) as the top-ranking structure. In the case of 4icb (Cal-binding D9 K), we also see that calcium ions are integral to the native structure, consistent with the pattern of failure observed in the previous set. In this instance, PBSA identified a structure 12 Å away from the native structure as the top-ranking structure.

In the Baker CASP3 set, although PBSA misidentified 1bg8-A and 1bl0, the native structures were still ranked as the number 2 candidates. In contrast, both GB and PBSA failed significantly in the case of 1eh2, which is another calcium-binding protein. The top-ranking decoys of 1eh2 in both scoring functions were ~10 Å away from the experimental structure. However, this is also a case under the influence of metal ion binding.

In the globin-homology set (hg_structal), the trend of failure is not so clear-cut, although PBSA and GB failed on almost identical sets of proteins. Here, the most native structures contain some ligand groups such as heme, the acetyl group, cyanide ion, etc. Therefore, binding of these ligands could have played roles. Nevertheless, PBSA performed slightly better than GB (69% vs. 65% accurate) on this set. On average, the native structures were also ranked slightly higher in PBSA than in GB. However, in the instance, where PBSA correctly identified the native structure but GB failed (2dhb-B), the top-ranking structure in GB was only 2.2 Å away from the experimental structure.

In the lattice ssfit decoy set containing conformations of eight small proteins generated by ab initio methods, PBSA correctly identified all the native structures, while GB misidentified one protein's (1nkl) native structure. It is interesting to note that this misidentified structure does not contain any bound ions or ligands and the top-ranking decoy in GB is about 10.4 Å away from the experimental structure.

In the local-minima decoy set, which contains conformations of ten proteins derived from the experimental secondary structures of a group of diverse structures, GB and PBSA correctly predicted the same number of native structures.

Finally, in the Lu and Skolnick set [21, 22] (courtesy of Lu and Skolnick), both GB and PBSA were able to identify the native structures correctly in all the decoy ensembles. Note that in our previous GB scoring using non-standard values for GB parameters, four native structures were misidentified. It appears that the default values for GB as found in the AMBER 7 package are more suited to scoring decoys generated by the threading-based tertiary restraints approach of Skolnick et al. [23].

Comparison of "*z*-scores"

The "*z*-score" is a statistical measure that tells how far and in what direction a given item deviates from the average of a distribution. It is defined as:

Table 7 Ranking statistics of Lu and Skolnick decoy set

PDB	N_{res}	RMSD	N_{decoy}	PBSA					GB				
				Rank	z	z'	R	R_s	Rank	z	z'	R	R_s
1a32	85	11.0∼16.2	96	1	−2.70	−1.92	0.24	−0.07	1	−2.03	−1.52	0.23	0.08
1ah9	71	5.3∼11.2	97	1	−6.95	−5.33	0.43	0.16	1	−6.23	−3.96	0.45	0.20
1aoy	78	3.6∼12.2	134	1	−7.35	−5.38	0.39	0.19	1	−6.64	−4.81	0.31	0.11
1bq9A	53	6.1∼11.1	115	1	−6.59	−4.63	0.34	0.08	1	−6.62	−4.62	0.33	0.04
1bw6A	56	4.2∼12.0	120	1	−4.04	−1.59	0.18	0.07	1	−5.08	−3.24	0.21	0.08
1c5a	66	4.3 ∼12.2	110	1	−8.09	−6.56	0.31	0.14	1	−6.96	−4.93	0.29	0.17
1cewI	108	4.8∼12.3	204	1	−7.49	−5.62	0.30	0.05	1	−3.56	−2.72	0.06	−0.02
1cis	66	3.4∼9.2	109	1	−5.60	−3.53	0.33	−0.02	1	−4.71	−2.68	0.22	−0.14
1csp	64	4.0∼11.9	145	1	−7.66	−5.41	0.07	−0.14	1	−6.97	−5.52	−0.06	−0.23
1erv	105	2.2∼13.3	88	1	−7.84	−6.16	0.70	0.29	1	−6.93	−5.22	0.65	0.29
1fas	61	3.4∼8.2	114	1	−7.58	−5.78	0.38	0.29	1	−2.40	−1.73	0.04	0.25
1ftz	70	4.6∼11.0	145	1	−6.66	−4.10	0.32	0.45	1	−2.26	−1.41	0.17	0.46
1gpt	47	2.3∼9.5	123	1	−4.57	−2.26	0.06	−0.06	1	−5.84	−3.81	0.09	−0.04
1hlb	138	2.4∼13.8	92	1	−7.94	−6.34	0.35	0.23	1	−6.80	−5.41	0.33	0.19
1hmdA	113	2.4∼12.0	99	1	−7.50	−6.41	0.45	0.15	1	−6.57	−5.18	0.43	0.21
1hp8	68	2.9∼13.0	109	1	−6.68	−4.95	0.16	0.01	1	−6.18	−3.98	0.11	−0.02
1ixa	39	3.4∼10.5	356	1	−3.57	−1.18	0.11	0.09	1	−4.77	−2.32	0.08	
1kjs	74	4.2∼13.4	119	1	−4.53	−2.47	0.13	0.11	1	−4.88	−2.55	0.17	0.16
1ksr	100	4.0∼8.9	224	1	−3.73	−1.17	0.08	−0.01	1	−5.25	−3.32	0.19	0.06
1lea	72	2.6∼6.4	137	1	−8.84	−7.31	0.52	0.14	1	−8.09	−6.44	0.47	0.14
1mba	146	2.2∼13.5	93	1	−8.03	−6.64	0.39	0.21	1	−3.94	−3.00	0.23	0.30
1ner	74	7.4∼13.6	105	1	−5.85	−3.63	0.35	0.13	1	−5.86	−3.38	0.31	0.09
1ngr	85	2.5∼13.6	84	1	−7.35	−6.01	0.25	0.10	1	−6.75	−4.60	0.31	0.18
1nkl	78	2.7∼16.5	78	1	−5.82	−3.29	0.35	0.28	1	−6.28	−4.69	0.28	0.17
1pdo	121	6.3∼11.1	124	1	−7.40	−5.16	0.56	0.43	1	−8.24	−6.41	0.61	0.42
1pgx	56	2.0∼11.4	73	1	−6.95	−5.61	0.17	0.00	1	−6.41	−5.01	0.35	0.17
1poh	85	1.8∼12.2	97	1	−7.61	−5.95	0.24	0.16	1	−6.64	−4.73	0.20	0.11
1pou	71	2.9∼10.6	88	1	−7.09	−5.28	0.35	0.08	1	−6.44	−4.46	0.35	0.07
1pse	69	7.8∼13.4	329	1	−8.33	−5.69	0.18	0.71	1	−6.09	−3.29	0.01	0.63
1rip	81	8.6∼15.6	433	1	−3.00	−0.36	0.02	−0.07	1	−4.38	−1.93	0.16	0.07
1rpo	61	7.3∼24.4	105	1	−7.13	−4.84	0.32	−0.02	1	−7.06	−5.41	0.25	−0.03
1shaA	103	2.2∼5.4	161	1	−8.36	−6.63	0.50	0.19	1	−7.78	−6.14	0.46	0.19
1shg	57	3.6∼9.5	86	1	−6.59	−4.62	0.31	0.00	1	−6.61	−5.13	0.30	−0.01
1sro	66	5.2∼12.4	98	1	−6.08	−4.09	0.36	0.01	1	−5.62	−4.00	0.32	−0.05
1stfI	98	5.3∼21.0	190	1	−1.59	−0.76	−0.01	0.08	1	−1.24	−0.46	−0.02	0.04
1thx	108	2.2∼3.7	88	1	−8.41	−7.22	0.53	−0.12	1	−7.68	−6.48	0.45	−0.16
1tit	89	2.0∼10.2	73	1	−5.66	−4.30	0.27	0.23	1	−4.97	−3.53	0.26	0.21
1tlk	103	3.4∼17.2	136	1	−5.14	−3.18	0.19	0.14	1	−6.36	−4.74	0.18	0.13
1ubi	76	1.9∼4.9	122	1	−9.03	−7.61	0.45	0.02	1	−7.72	−5.85	0.35	−0.01
1vif	60	2.6∼11.5	111	1	−8.36	−6.68	0.31	0.28	1	−7.08	−5.36	0.24	0.21
1wiu	93	2.3∼12.5	103	1	−5.49	−3.63	0.36	0.37	1	−4.17	−2.16	0.29	0.31
2af8	86	3.5∼12.6	144	1	−4.28	−1.81	0.28	0.04	1	−5.69	−3.30	0.25	−0.01
2azaA	129	4.2∼13.0	121	1	−8.86	−7.52	0.08	−0.13	1	−7.71	−6.19	0.07	−0.03
2bby	69	2.9∼12.8	92	1	−6.16	−4.43	0.20	0.08	1	−6.19	−4.46	0.22	0.06
2ezh	65	3.5∼13.0	110	1	−7.02	−5.34	0.18	−0.01	1	−6.54	−4.71	0.19	−0.05
2ezk	93	4.0∼15.4	82	1	−7.00	−5.58	0.56	0.28	1	−6.83	−5.62	0.52	0.25
2fmr	65	3.3∼11.1	128	1	−6.59	−4.75	0.19	0.09	1	−5.91	−4.13	0.17	0.12
2lfb	100	11.1∼16.5	228	1	−6.87	−4.23	0.24	0.07	1	−7.01	−4.58	0.27	0.10
2pcy	99	1.7∼12.0	71	1	−6.71	−5.39	0.32	0.17	1	−6.48	−5.38	0.27	0.09
2ptl	60	2.4∼12.9	122	1	−5.42	−2.55	0.26	0.17	1	−5.18	−3.19	0.21	0.14
2sarA	96	4.8∼13.5	125	1	−5.50	−3.32	0.26	0.26	1	−6.66	−4.64	0.29	0.28
5fd1	106	9.3∼15.2	143	1	−4.47	−2.64	0.21	0.03	1	−7.52	−5.89	0.32	−0.05
6pti	57	3.2∼11.3	156	1	−7.56	−5.57	0.25	−0.06	1	−6.82	−5.24	0.28	0.02
Average	82	4.1∼12.3	133		−6.45	−4.57	0.29	0.12		−5.94	−4.22	0.26	0.11

$$z_{native} = \frac{x_{native} - \bar{x}}{\sigma} \quad (4)$$

where x is the energy score of the native structure, $\bar{x}$ is the average energy score of the decoy ensemble and σ is the standard deviation of the decoy ensemble. Because it is desirable for a scoring function to be able to separate the native state as far apart from the non-native states, the z-scores is often used to assess this aspect of scoring functions.

In this benchmark, the average z-score ranges from −0.53 to −6.45 for the PBSA scores, and from −0.29 to −5.94 for the GB scores. In all but the local minima decoy set (LMDS), PBSA scores resulted in a better average value of z-score than GB scores. This result suggests that the use of PBSA has captured (and perhaps

Table 8 List of incorrectly identified structures

		PBSA	GB
4 state reduced	3icb	*	*
	4rxn	*	
Fisa	*1ctf*	*	*
	1hdd-C	*	*
	4icb	*	
Baker CASP3	1bg8-A	*	
	1bl0	*	
	1eh2	*	*
Hg_structal	*1hlb*	*	*
	1hlm	*	*
	1hsy	*	*
	1mbs	*	*
	1myg-A	*	*
	1myj-A	*	*
	2dhb-A	*	*
	2pgh-A	*	*
	2pgh-B	*	*
Lattice ssfit	1nkl		*
LMDS	*1bo0n-B*	*	*
	1bba	*	*
	1dtk	*	
	1fc2		*

The "*" indicates that the method failed to identify the native structure from decoys

amplified) certain common distinguishing properties of the native state, and in this respect, the use of PBSA in the scoring function has improved upon the GB scores.

In another related comparison, which we call z', we examined the separation between the native state and the best-ranking decoy in standard-deviation units. z' is defined as:

$$z' = \frac{x - x'}{\sigma} \tag{5}$$

where x is the score of the native state, x is the score of the best-ranking decoy, and σ is the standard deviation of the decoy scores. This measure defines the lower bound of the decoy distribution in terms of the distance between the lowest-energy decoy and the average energy of the ensemble in standard-deviation units. In the z-score comparison, we asked how far the native state is from the center of the decoy distribution. An interesting question to ask here is how well separated the native state is from the edge of the distribution. Because the main difference in the two scoring functions is in the treatment of solvation energy, our interpretation here is that the greater value of z signifies the greater sensitivity of the native state to solvation effect. Here, we see in Table 9 that the differences between the PBSA and GB are small in general. In the case of the local-minima decoy set, the native structures are sensitive to these two different methods of solvation-energy treatment and the two different solvation schemes resulted in about 1.0 standard deviation difference in the native structure scores in favor of GB. This is also true for "lattice ssfit" set, albeit in the opposite direction. Thus, while a more sophisticated treatment of solvation effect is expected to improve the scoring result, this is not universally true and in most cases, the performance of GB and PBSA were comparable.

Correlations to Cα-RMSD

For the purpose of structure prediction, a good correlation between the energetic scores and a similarity-distance measure is a desirable characteristic. In Table 1, 2, 3, 4, 5, 6, and 7, we listed the Pearson correlation (R) and Spearman's rank-order correlation (R_s) between the C_α-RMSD of decoys from the native structure to their respective energy scores. The average values ranged from −0.01 to 0.63. In general, the RMSD-energy correlation of the PBSA scoring function was comparable to that of the GB scoring function (0.19 for PBSA and 0.16 for GB) and neither appeared to be significant.

Looking closer at the issue of correlation, it is generally recognized that as a consequence of the rugged

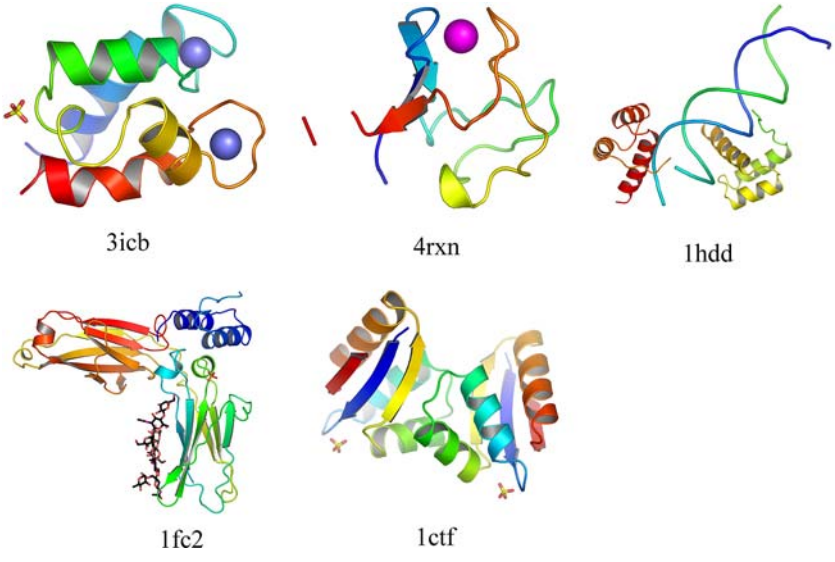

Fig. 1 Experimental structures of incorrectly predicted structures

Table 9 Comparison of z-scores

	PBSA		GB		Difference	
	z	z'	z	z'	$z_{PB}-z_{GB}$	$z'_{PB}-z'_{GB}$
4 state reduced	−2.41	−0.55	−2.22	−0.88	−0.19	0.33
Fisa	−0.53	0.42	−0.29	0.09	−0.24	0.33
Baker CASP3	−1.01	−0.18	−0.65	−0.15	−0.36	−0.03
hg_structal	−1.6	−0.37	−1.53	−0.45	−0.07	0.08
lattice ssfit	−2.62	−1.22	−1.46	−0.57	−1.16	−0.65
Lmds	−2.12	−0.04	−3.64	−0.94	1.52	0.90
Lu and Skolnick	−6.45	−4.57	−5.94	−4.22	−0.51	−0.35
Average	−3.9	−2.29	−3.67	−2.21	−0.14	0.09

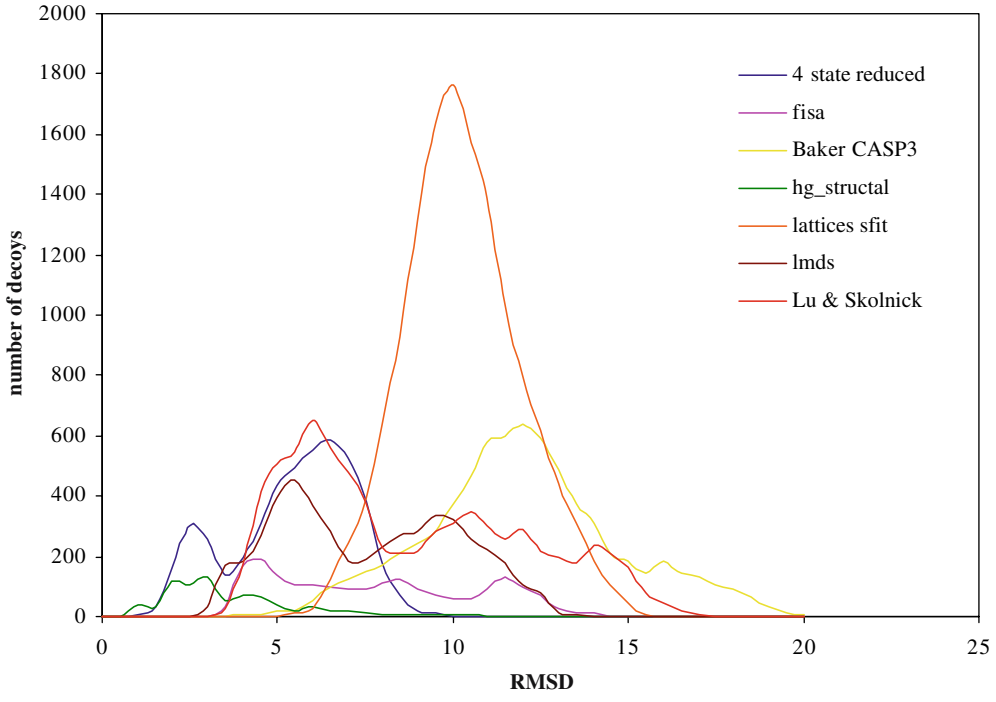

Fig. 2 Distribution of decoys with respect to their RMSD from the native state

energy landscape, small deviations in C_α-RMSD may result in large differences in energy and vice versa. Furthermore, in a recent work, Kihara et al. [24] conducted an extensive comparison of all representative structures in the PDB and found that a large number of proteins can be aligned to unrelated folds with RMSD as small as 3.5 Å. Thus, using C_α-RMSD as a measure for similarity beyond a small range does not appear to be a meaningful practice. One interesting observation from our results is that in the globin-homology set (hg_structal), the correlation coefficients stand out as the most highly correlated data set. In Fig. 2, we plotted the distribution of decoys in each set with respect to their C_α-RMSD from the native state. Most of the decoys are distributed beyond 5 Å C_α-RMSD. The only exception is the hg_structal set, which has most decoys below 5 Å C_α-RMSD. This observation reflects the fact that hg_structal decoys were generated by comparative homology-modeling methods, whereas decoys in other data sets were produced using *ab initio* methods that samples the conformational space in an energy-guided rather than structure-guided fashion.

Comparison to Hsieh and Luo scoring function

In our final comparison, we look at the recent results obtained by Hsieh and Luo [10] in which they also scored similar sets of decoys with a similarly designed scoring function. In their study, the AMBER molecular-mechanics force field and molecular-dynamics simulations were also used to obtain the energetic scores. The main differences between these two approaches are the force-field parameter set used and the treatment of solvent effect. In their approach, they incorporated the PB solvent model directly into the molecular-dynamics simulation and simulated the protein dynamics in PB solvent, whereas in our approach, the molecular-dynamics simulations were carried out in GB solvent and the PBSA energetic contributions were estimated by

post-processing the resulting molecular-dynamics trajectories. The advantage of our approach is that, once the improved accuracy of PBSA scoring over GB is established, one can selectively perform the time-consuming PBSA calculations only on the top-ranking decoys identified from the GB simulations, as opposed to having to perform PBSA calculations on all decoys.

Tables 10 and 11 list the side-by-side comparison of native rankings in the two decoy sets used in both of the two studies. In Table 10, the 4-state reduced decoy set, our post-processing PBSA approach clearly performed worse than the direct PB approach of Hsieh and Luo, and in Table 11, the globin-homology decoy set, our approach performed comparably to the direct PB approach. Overall, it appears that in terms of the ability to identify the correct native structure from among the decoy ensemble, the two approaches performed at comparable levels, although the direct PB approach improved the average z-scores over the post-processing approach.

A potential bias can arise in earlier comparisons in which trajectories were generated from GB simulations. Indeed, comparisons based on explicit-solvent simulations could eliminate this potential bias. Alternatively, replacing GB solvent with PB solvent directly in the MD simulations might also overcome the problem. To this end, it is interesting to note that neither the post-processing nor the direct PB approaches outperformed the GB-based scoring approach significantly.

It is rather encouraging to note that physics-based scoring approach has come a long way. Although the earlier studies based on gas-phase energies laid the

Table 10 Comparison with Hsieh and Luo scoring function (4 state reduced)

PDB	N_{decoy}	Post-processing PB		Direct PB		GB	
		Rank	z	Rank	z	Rank	z
1ctf	631	1	−3.00	1	−2.76	1	−1.70
1r69	676	1	−2.89	1	−3.01	1	−1.89
1sn3	661	1	−1.84	1	−4.88	1	−1.14
2cro	675	1	−1.99	1	−2.58	1	−1.54
3icb	654	*7*	*−1.34*	*2*	*−2.06*	*2*	*−0.80*
4pti	688	1	−3.63	1	−4.77	1	−3.46
4rxn	678	*6*	*−2.20*	1	−3.95	1	−5.00
Average			−2.41		−3.43		−2.22

The incorrectly identified entries are highlighted

Table 11 Comparison with Hsieh and Luo scoring function (hg_structal)

PDB	N_{res}	Post-process PB		Direct PB		GB	
		Rank	z	Rank	z	Rank	z
1ash	147	1	−2.34	1	−4.32	1	−2.85
1bab-B	146	1	−2.76	1	−2.5	1	−2.48
1col-a	197	1	−3.20	1	−2.73	1	−1.53
1cpc-A	162	1	−4.41	1	−4.42	1	−4.42
1ecd	136	1	−0.97	1	−1.29	1	−0.71
1emy	153	1	−1.29	1	−1.43	1	−0.89
1flp	142	1	−2.88	1	−3.47	1	−3.29
1gdm	153	1	−1.17	1	−1.63	1	−0.81
1hbg	147	1	−2.76	1	−3.57	1	−3.23
1hbh-A	142	1	−1.93	*2*	*−2.4*	1	−3.23
1hbh-B	146	1	−1.90	1	−2.75	1	−2.01
1hda-A	141	1	−1.63	1	−2.3	1	−1.85
1hda-B	145	1	−2.33	*2*	*−2.7*	1	−2.11
1hlb	157	*6*	*−0.85*	*4*	*−4.19*	*5*	*−0.79*
1hlm	158	*28*	*0.29*	*28*	*−1.23*	*29*	*0.15*
1hsy	153	*5*	*−0.87*	*2*	*−0.95*	*2*	*−0.60*
1ith-A	146	1	−0.92	1	−1.56	1	−0.55
1lht	153	1	−1.03	1	−1.58	1	−0.69
1mba	13	1	−2.44	1	−3.01	1	−2.61
1mbs	153	*29*	*1.52*	*25*	*−1.44*	*29*	*0.73*
1myg-A	153	*4*	*−0.95*	*3*	*−1.65*	*4*	*−0.68*
1myj-A	153	*4*	*−1.76*	*2*	*−2.14*	*5*	*−1.57*
1myt	146	1	−0.97	1	−1.41	1	−0.72
2dhb-A	141	*8*	*−0.67*	*4*	*−2.27*	*13*	*−0.41*
2dhb-B	146	1	−2.05	1	−2.18	*18*	*0.09*
2lhb	149	1	−2.86	1	−3.02	1	−3.06
2pgh-A	141	*16*	*−0.13*	*5*	*−2.28*	*14*	*−0.40*
2pgh-B	146	*8*	*−0.35*	*4*	*−1.31*	*8*	*−0.34*
4sdh-A	145	1	−2.83	1	−4.04	1	−3.47
Average			−1.60		−2.41		−1.53

Incorrectly identified entries are marked in italics

groundwork for much of the work cited herein, inclusion of solvation effects has been a crucial step in the development of physics-based scoring methods. Some of the clear advantages of the physics-based scoring functions are consistency, repeatability, and transferability. Although performance differences do exist, most of the physics-based scoring functions have been shown to do a reasonable job, despite the considerable differences in the details. This is a rather encouraging feature and is expected to facilitate wide applications in the community.

One the other hand, this study also points to the weaknesses in this type of method, one of which is the poor scoring performance in the ion-bound proteins. Admittedly, this is a rather difficult issue because atomic-level information is needed to model the ions accurately. However, the present scoring methods are rather generic. Another area that may need improvement is the conformational-sampling ability. This was clearly the case for 1hdd, in which the native experimental structure is a DNA-protein complex and in the "hg" decoy set, in which most native experimental structures were holo-complexes with rather large ligands. However, the decoys were in the apo forms. Evidently, considerable conformational changes are expected between the apo- and the holo-forms and energetic comparison between these two forms has to be made within this context. In these cases, interactions with ligands and substrates play important roles and correct scoring functions must take these interactions into account. Conversely, it is most likely unfruitful without considering the ligands. To some extent, scoring against these apo-decoys is a bit misleading. As a consequence, the inability of scoring these proteins is not necessarily a disapproval of the scoring methods or functions.

Conclusions

In this study, we have attempted to examine the MM-PBSA method of free-energy estimation by comparing the results against a GB-based approach using large protein-decoy datasets. The PB-based approach offers a clear conceptual advantage. However, the overall performance of the MM-PBSA approach is comparable to the computationally less expensive GB approach. This is further corroborated by the direct comparison of our results to those obtained by Hsieh and Luo using a direct PB solvent simulation, which also showed marginal improvement over the GB method.

This result led us to conclude that PB-based approaches provide a slight improvement upon GB-based scoring functions. Obviously, the disadvantage of the PB-based approach is the increased computational cost. To this end, methods such as those used by Hsieh and Luo are important for the application of the PB-based approach. On the other hand, the constant improvement in the GB method will also bring about the changes needed for a higher level performance without incurring the computational cost associated with the PB method.

A second conclusion of this study is that, in order to characterize scoring functions better, a better similarity measure than C_α-RMSD is required. Recently, Zhu et al. [25] have demonstrated that using the content of native inter-residue contacts as the similarity measure can substantially increase the correlation between similarity distance and the energy scores. Several new similarity measures such as the graph-theory based method of Weskamp et al. [26] or the topological representation of Bostick et al. [27] have been developed to facilitate comparison of protein structures at the genomic scale. We believe that co-development of future scoring functions and similarity-measurement methods might be a fruitful synergistic combination.

Acknowledgements We are grateful for the decoy sets provided by various groups. This work was supported by research grants from NIH (GM64458 and GM067168 to YD).

References

1. Cornell WD, Cieplak P, Bayly CI, Goulg IR, Merz KM, Ferguson DM, Spellmeyer DC, Fox T, Caldwell JW, Kollman PA (1995) J Am Chem Soc 117:5179–5197
2. Jorgensen WL, Tirado-Rives J (1988) J Am Chem Soc 110:1657–1666
3. Lazaridis T, Karplus M (1999) Proteins 35:133–152
4. Lazaridis T, Karplus M (1999) J Mol Biol 288:477–487
5. Fan ZZ, Hwang J-K, Warshel A (1999) Theor Chem Acc 103:77–80
6. Vorobjev YN, Hermans J (1999) Biophys Chem 78:195–205
7. Feig M, Brooks CL III (2002) Proteins 49:232–245
8. Dominy B, Brooks C (2002) J Comput Chem 23:147–160
9. Felts AK, Gallicchio E, Wallqvist A, Levy RM (2002) Proteins 48:404–422
10. Hsieh M-J, Luo R (2004) Proteins 56:475–486
11. Duan Y, Wu C, Chowdhury S, Lee MC, Xiong G, Zhang W, Yang R, Cieplak P, Luo R, Lee T, Caldwell J, Wang J, Kollman P (2003) J Comput Chem 24:1999–2012
12. Lee MC, Duan Y (2004) Proteins 55:620–634
13. Srinivasan J, Miller J, Kollman PA, Case DA (1998) J Biomol Struct Dyn 16:671–682
14. Sitkoff D, Sharp KA, Honig B (1998) J Phys Chem 98:1978–1983
15. Darden TA, York DM, Pedersen LG (1993) J Chem Phys 98:10089–10092
16. Reyes CM, Kollman PA (1999) RNA 5:235–244
17. Cheatham III TE, Kollman PA (1996) J Mol Biol 259:434–444
18. Kuhn B, Kollman PA (2000) J Med Chem 43:3786–3791
19. Chong LT, Duan Y, Wang L, Massova I, Kollman PA (1999) Proc Natl Acad Sci USA 96:14330–14335
20. Park B, Levitt M (1996) J Mol Biol 258:367–392
21. Lu H, Skolnick J (2001) Prot-Struct Funct Genet 44:223–232
22. Lu L, Lu H, Skolnick J (2002) Prot-Struct Funct Genet 49:350–364
23. Kihara D, Lu H, Kolinski A, Skolnick J (2001) Proc Natl Acad Sci USA 98:10125–10130
24. Kihara D, Skolnick J (2003) J Mol Biol 334:793–802
25. Zhu J, Zhu Q, Shi Y, Liu H (2003) Proteins 52:598–608
26. Weskamp N, Kuhn D, Hullermeier E, Klebe G (2004) Bioinformatics 20:1522–1526
27. Bostick DL, Shen M, Vaisman II (2004) Proteins 56:487–501